

## Supporting Information

### **Metal-Free Boron Nanosheet as “Buffer Electron Pool” for Urea and Ethanol Synthesis via C–N and C–C Coupling**

*Yongyong Cao<sup>a</sup>, Yuxiao Meng<sup>a,b</sup>, Yuting Wu<sup>a</sup>, Hongjie Huang<sup>a,b</sup>, Weichan Zhong<sup>a,c</sup>,  
Zhangfeng Shen<sup>a</sup>, Qineng Xia<sup>a</sup>, Yangang Wang<sup>a\*</sup>, Xi Li<sup>a\*</sup>*

- a. College of Biological, Chemical Science and Engineering Jiaying University, Jiaying, Zhejiang, 314001 (P. R. China).*
- b. Institute of Industrial Catalysis, College of Chemical Engineering, State Key Laboratory Breeding Base of Green-Chemical Synthesis Technology, Zhejiang University of Technology, Hangzhou 310032 (P. R. China)*
- c. Key Laboratory of the Ministry of Education for Advanced Catalysis Materials, Institute of Physical Chemistry, Zhejiang Normal University, Jinhua 321004 (P. R. China)*

## Computational Details

### 1 The adsorption energy and reaction Gibbs Free Energy Calculations

The adsorption energy ( $E_{\text{ads}}$ ) of all intermediates was defined as:

$$E_{\text{ads}} = E_{\text{adsorbates+cat}} - E_{\text{adsorbates}} - E_{\text{cat}} \quad (1)$$

where  $E_{\text{adsorbates+cat}}$ ,  $E_{\text{adsorbates}}$ , and  $E_{\text{cat}}$  correspond to the energies of adsorbates on the surface of  $\beta_{12}$ -BM, the free adsorbates, and the  $\beta_{12}$ -BM catalyst using DFT calculations, respectively.

The change in Gibbs free energy ( $\Delta G$ ) for the adsorbed species is calculated from the following equation:

$$\Delta G = \Delta E_{\text{DFT}} + \Delta E_{\text{ZPE}} - T\Delta S \quad (2)$$

Where  $\Delta E_{\text{DFT}}$  is the reaction energy calculated based on DFT calculations,  $\Delta E_{\text{ZPE}}$  and  $T\Delta S$  are the zero-point energy correction and entropy contributions,  $T$  is the temperature. Entropy values of gaseous molecules, such as  $\text{H}_2$ ,  $\text{NO}$ ,  $\text{CO}_2$ ,  $\text{CO}$ , and  $\text{NH}_3$ , are taken from the standard tables in *Physical Chemistry*.

In the computational hydrogen electrode (CHE) model,<sup>1,2</sup> the chemical potential of proton-electron pair ( $\text{H}^+/\text{e}^-$ ) is equal to half of a hydrogen molecule at standard hydrogen electrode (SHE) conditions:

$$\Delta G(\text{H}^+/\text{e}^-) = 1/2 \Delta G_{\text{H}_2} - eU \quad (3)$$

The bias effect on the free energy is taken into account by shifting the energy of the state by:

$$\Delta G_{\text{U}} = -neU \quad (4)$$

where  $n$  is the number of  $\text{H}^+/\text{e}^-$  pairs transferred in the reaction.

$U_{\text{L}}$  is the highest potential where all of the steps are downhill in free energy.<sup>3</sup> It is calculated as:

$$U_{\text{L}} = -\Delta G/e \quad (5)$$

where  $\Delta G$  is the free energy of the potential-limiting step.

### 2. Selectivity Calculations

Since only two competitive reactions are considered according to the Boltzmann distribution in the formulation, it only can simply estimate the selectivity of reaction. However, the urea and the ethanol formation are complex reactions that involve multiple competitive hydrogen evolution reaction (HER), NO reduction reaction (NORR), and CO<sub>2</sub> reduction reaction (CO<sub>2</sub>RR) in this study. To solve this problem, the urea and ethanol formation main reaction, side reactions and  $\Delta G$  value of potential-determining step (PDS) of corresponding reactions are all listed in the Table S3. For urea formation, there are five competitive reactions, including H<sub>2</sub>, NH<sub>3</sub>, CO, CH<sub>4</sub> and CH<sub>3</sub>OH formation. The NH<sub>3</sub> formation is considered to be the dominant competitive reaction among above five reactions based on  $\Delta G$  value of PDS. Similarly, the selectivity of ethanol formation also is simply estimated by only considering CH<sub>4</sub> formation. Therefore, the selectivity of urea and ethanol according to Boltzmann distribution<sup>[4]</sup> can be defined as:

$$f = 1 / (1 + \exp \{-\delta G / k_B T\}) \quad (6)$$

Where  $\delta G$  is the Gibbs free energy difference between two competitive reactions,  $k_B$  is the Boltzmann constant, and  $T$  is the temperature. Considering the competitive formation of H<sub>2</sub> and NH<sub>2</sub>CONH<sub>2</sub> as an example, for instance, if the possibility of the formation of NH<sub>2</sub>CONH<sub>2</sub> is set as 1, the possibility of the formation of H<sub>2</sub> would be  $\exp \{-\delta G / k_B T\}$ , where  $\delta G = \Delta G_{H_2} - \Delta G_{NH_2CONH_2}$ . If  $\delta G$  is positive, the possibility of the formation of H<sub>2</sub> is less than 1, and its selectivity will be larger than 50%.

### 3. Slow-growth approach Calculations

The slow growth method is based on thermodynamic integration to compute the free energy profile along the reaction coordinates. Therefore, the constrained AIMD and the “slow-growth” approach were employed to evaluate the kinetic barriers to obtain the free-energy profile of C–N and C–C coupling along the collective variable (CV).<sup>5,6</sup> The free energy difference between two states (initial state (IS) and final state (FS)) can be calculated by thermodynamic integration as:

$$W_{FS} - W_{IS} = \int_{\xi(I)}^{\xi(F)} \frac{dF}{d\xi} d\xi \quad (7)$$

where  $F$  is the free energy;  $\frac{dF}{d\xi}$  is the potential of mean force, which is calculated along a constrained MD sampling; The CV value is used to limit the degree of freedom  $\xi$  in the phase space as the reaction coordinate. The work  $W_{FS} - W_{IS}$  corresponds to the free energy difference between the final and initial state. For the C-N coupling formation step, the CV is chosen as the reaction coordinate. The free energy samplings were performed with the CV value of the C-N bond distance ( $d_{C-N}$ ). A  $d\xi$  value of 0.0005 Å is used for each MD step after testing a shorter step size for the “slow-growth” along the reaction coordinate.

#### 4. Constant-potential Models

In this study, the electrode potential versus SHE was determined by referencing the work function of electrochemical interface to an experimental value of 4.44 eV for the SHE<sup>[7]</sup>. Then the electrode potentials of the  $\beta_{12}$ -BM surface were determined by:

$$U_{SHE} = (\phi - \phi_{SHE}) / e = (\phi - 4.44) / e \quad (8)$$

where  $\phi$  is the work function, which can be computed from DFT calculations. The work function values for  $\beta_{12}$ -BM with various C-N and C-C intermediates are summarized in Table S4. We considered the average value of the potential at the initial state ( $U_{IS}$ ) and transition state ( $U_{TS}$ ) as the potential ( $U_r$ ) of the reaction (i.e.,  $U_r = (U_{IS} + U_{TS})/2$ ). As shown in the Table S4, these data show that although the adsorbed intermediates are different, the computed electrode potentials of C-N and C-C intermediates are about 0.65 V vs SHE and 0.68 V vs SHE, respectively.

The constant potential correction method was used to get C-N and C-C electrochemical coupling barrier at constant potential developed by Chan and Nørskov<sup>[8]</sup>.

$$\Delta E = (\Delta q \cdot \Delta\phi) / 2 \quad (9)$$

where  $\Delta E$ ,  $\Delta q$ , and  $\Delta\phi$  corresponds to the energy correction due to change of electrode

potential, charges and workfunctions

## Supplementary Results

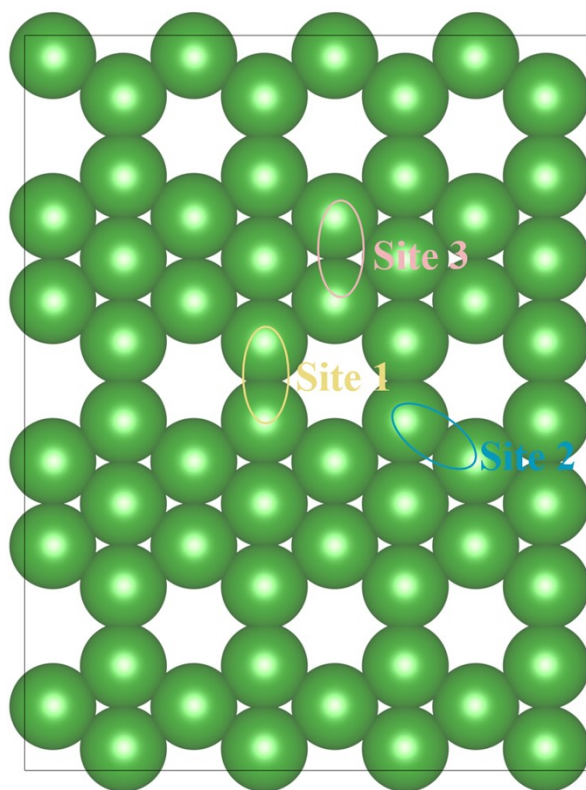


**Fig. S1** Top views of the atomic configurations of  $\beta_{12}$ -BM with three different active site for  $\text{CO}_2$  and  $\text{NO}$  molecule adsorption.

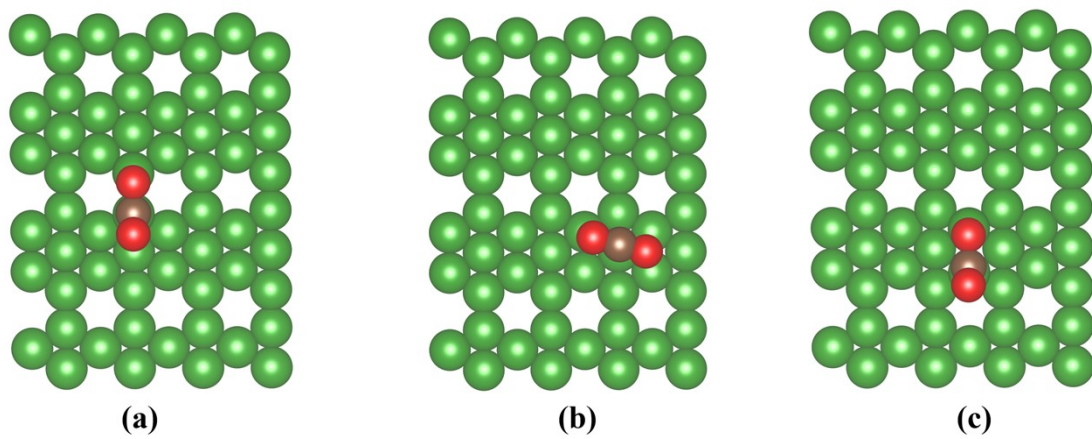


**Fig. S2** Top views of the atomic configurations of CO<sub>2</sub> adsorption on (a) site 1 (b) site 2 and (c) site 3 in  $\beta_{12}$ -BM.

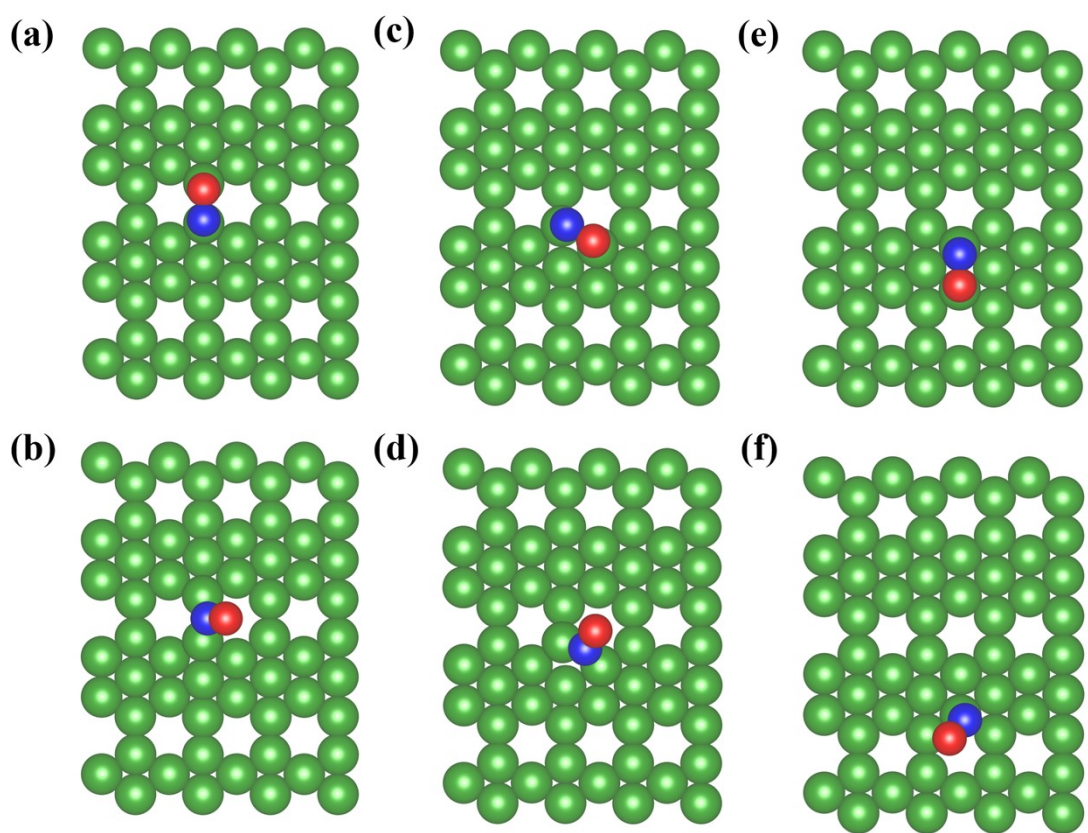


**Fig. S3** Top views of the atomic configurations of NO adsorption on (a) – (b) site 1, (c) – (d) site 2, and (e)-(f) site 3 in  $\beta_{12}$ -BM via side-on and end-on pattern, respectively.

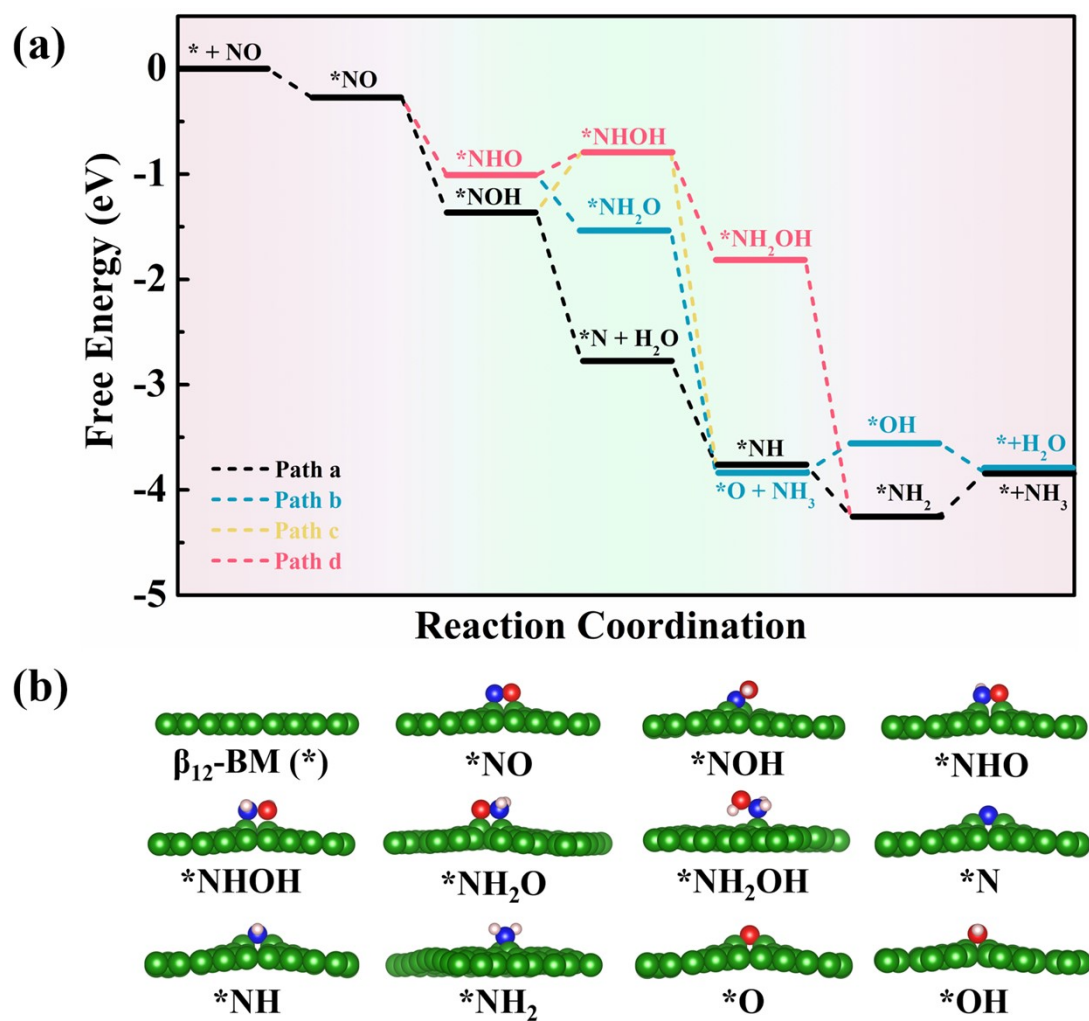


**Fig. S4** (a) Free energy profiles for the NORR on  $\beta_{12}$ -BM and (b) the corresponding configurations of all the possible intermediates



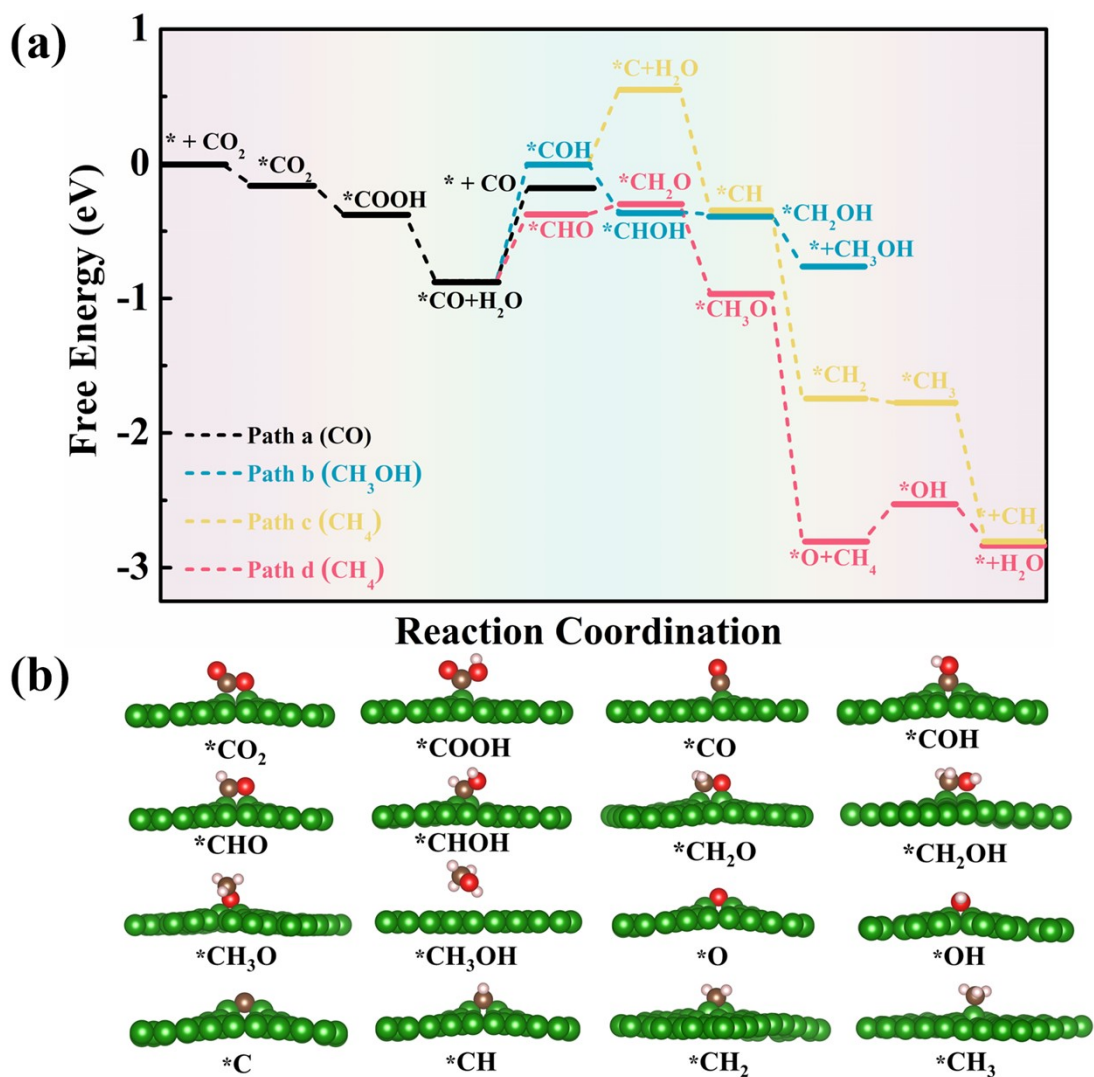


**Fig. S5** (a) Free energy profiles of the CO<sub>2</sub>RR for producing the C1 products on  $\beta_{12}$ -BM and (b) the corresponding configurations of all the possible intermediates

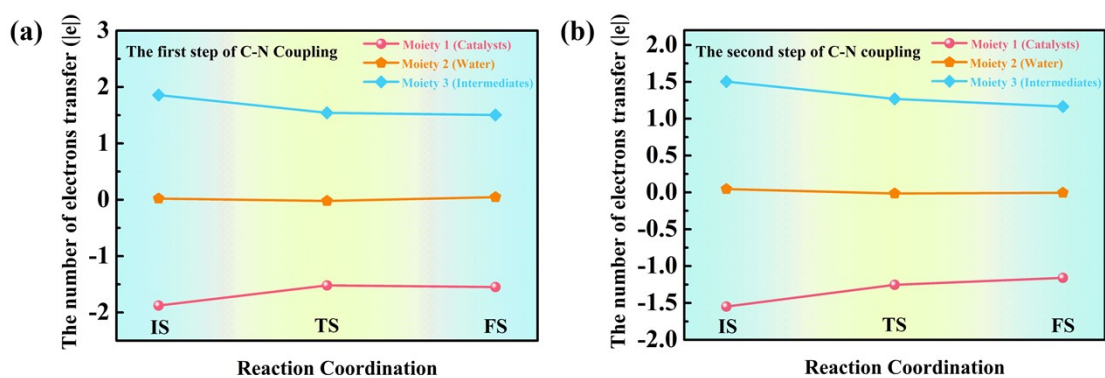


**Fig. S6** (a), (b) Charge variation of the three moieties along two steps of C-N coupling reactions. Moieties 1, 2, and 3 represent the  $\beta_{12}$ -BM surface, the water molecules, and the adsorbed species, respectively. The positive values represent the electron obtained; negative values represent the loss of electrons.

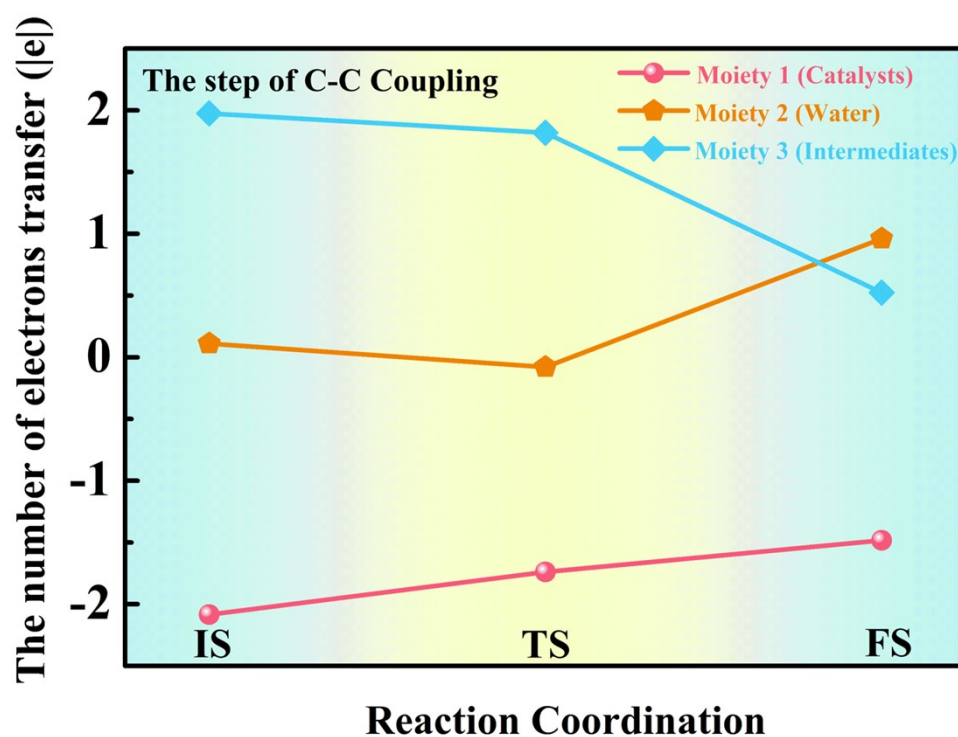


**Fig. S7** Charge variation of the three moieties along C-C coupling reactions. Moieties 1, 2, and 3 represent the  $\beta_{12}$ -BM surface, the water molecules, and the adsorbed species, respectively. The positive values represent the electron obtained; negative values represent the loss of electrons.

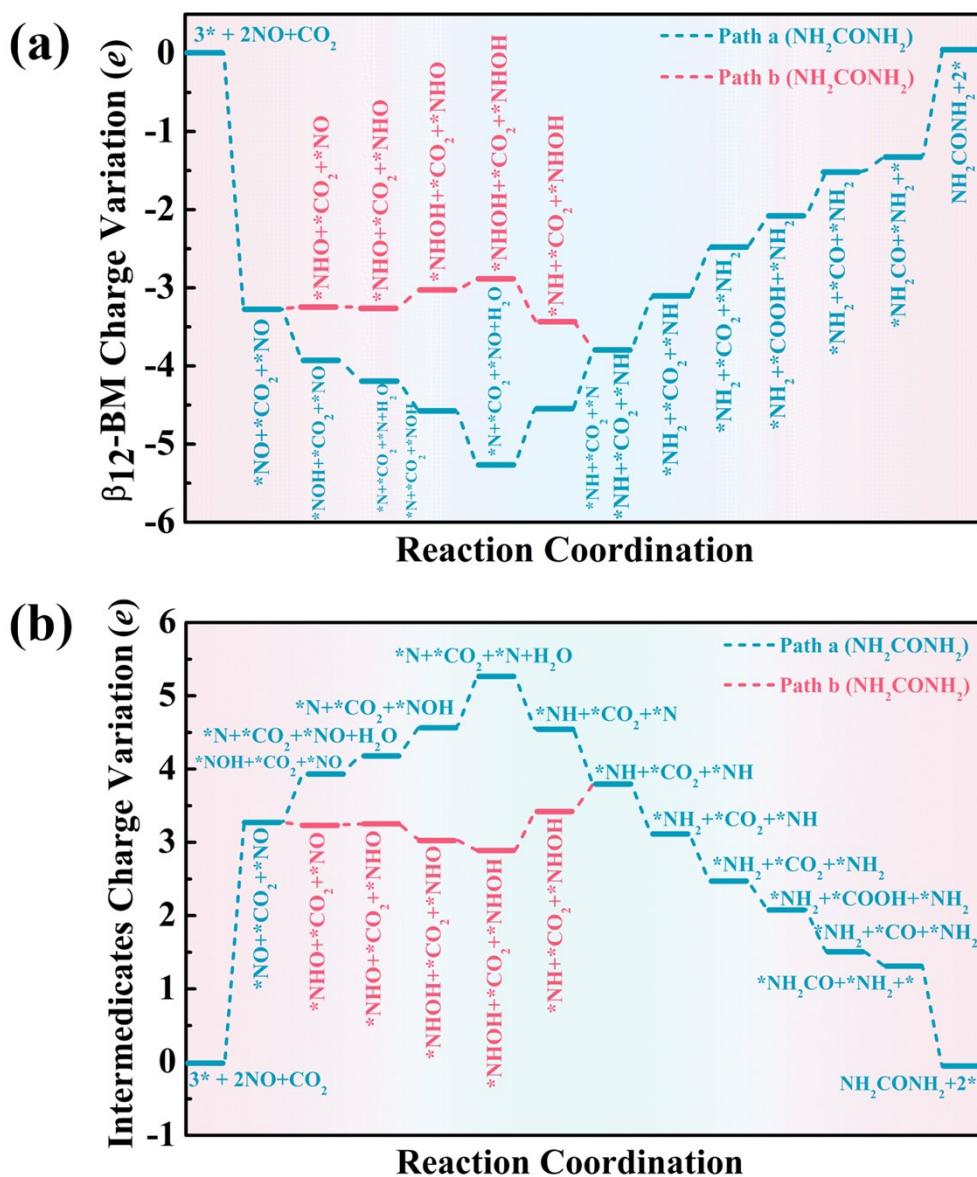


**Fig. S8** Charge variation of the (a)  $\beta_{12}$ -BM and (b) intermediates during the urea formation. The positive values represent that the intermediates gain electrons from  $\beta_{12}$ -

BM; the negative values represent the loss of electrons.

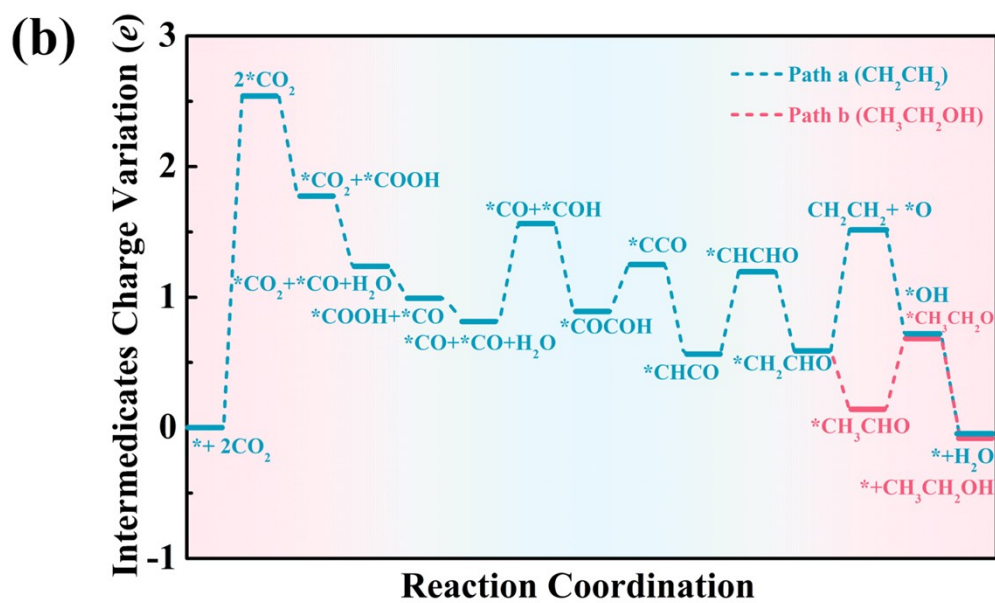
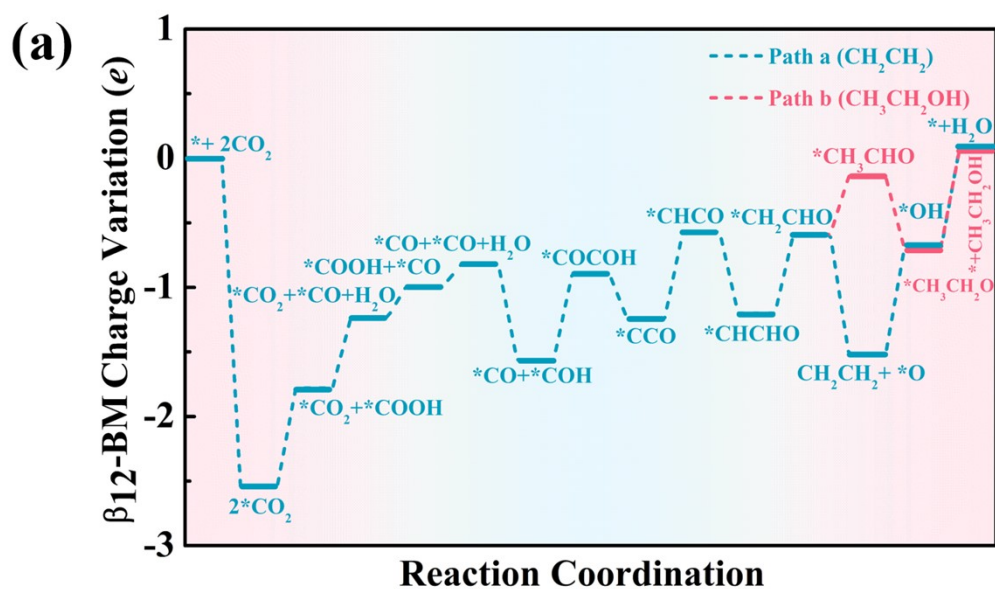


**Fig. S9** Charge variation of (a)  $\beta_{12}$ -BM and (b) intermediates during the ethanol formation. The positive values represent that the intermediates gain electrons from  $\beta_{12}$ -BM; the negative values represent the loss of electrons.

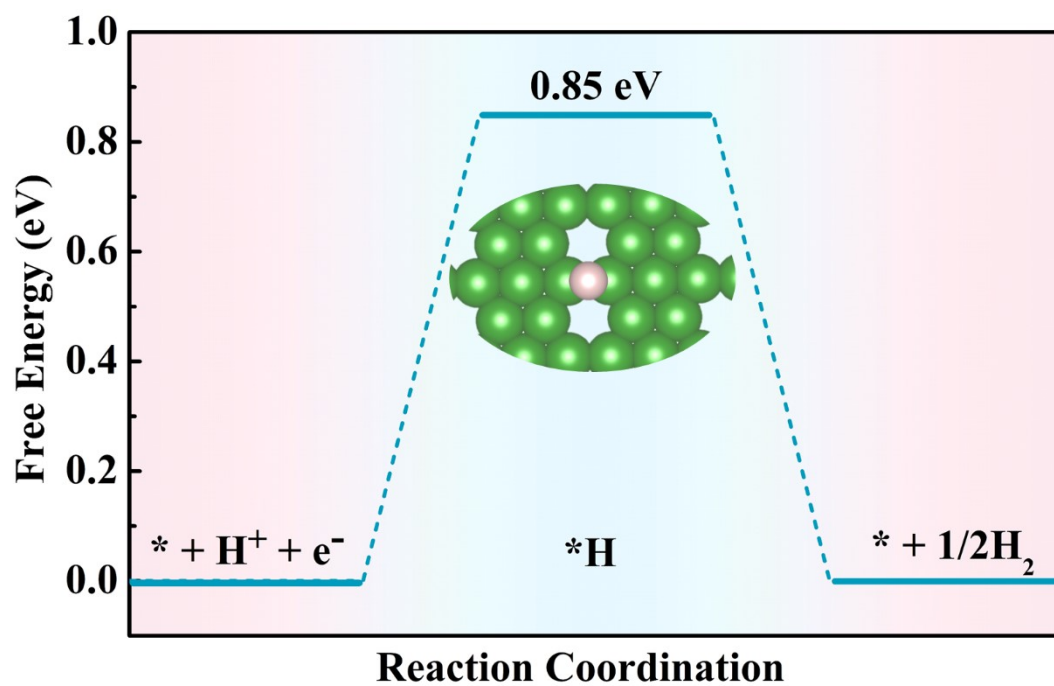


**Fig. S10** Free energy profiles and the corresponding configuration for the HER on  $\beta_{12}$ -BM.

Table S1. Workfunctions ( $\phi$ ) of initial state and transition state, average value of the potential and Energy correction for C-N and C-C coupling reaction

	Reaction Equation	$\phi$ values of IS (eV)	$\phi$ values of TS (eV)	Potential of reaction (V)	Energy correction (eV)
C-N Coupling	*CO+*NH <sub>2</sub> →*CONH <sub>2</sub>	5.16	5.03	0.66	0.04
	*CONH <sub>2</sub> +*NH <sub>2</sub> →*NH <sub>2</sub> CONH <sub>2</sub>	5.12	5.02	0.63	0.03
C-C coupling	*CO+*COH→*COCO	5.10	5.13	0.68	0.01

**Table S2.** The adsorption energy of the adsorbed CO<sub>2</sub> and NO molecules ( $E_{ads}$ ), the angle of adsorbed CO<sub>2</sub> (degree) and the bond length of adsorbed NO (Å) in the gas phase and liquid phase for  $\beta_{12}$ -BM.

	Gas phase			Liquid phase		
	$E_{ads}$ (eV)	Angle of CO <sub>2</sub> (degree)	Bond length of N-O (Å)	$E_{ads}$ (eV)	Angle of CO <sub>2</sub> (degree)	Bond length of N-O (Å)
*CO <sub>2</sub>	-0.54	127.23	---	-4.47	124.72	--
*NO	-0.87	---	1.31	-5.93	---	1.45/1.41
*CO <sub>2</sub> _2*CO <sub>2</sub>	-0.53/	125.04/121.54	---	-5.34/	122.11/118.3	---
	-0.54			-5.42		
*CO <sub>2</sub> _2*NO	-0.54/	126.11	1.32/1.31	-4.47/	120.82	1.46





## References

- (1) J. Nørskov, J. Rossmeisl, A. Logadottir, L. Lindqvist, J.R. Kitchin, T. Bligaard and H. Jonsson, *J. Phys. Chem. B* 2004, **108**, 17886–17892.
- (2) H. Li, S. Kelly, D. Guevarra, Z. Wang, Y. Wang, J. A. Haber, M. Anand, G. T. K. K. Gunasooriya, C. S. Abraham and S. Vijay, *Nat. Catal.* 2021, **4** (6), 463-468.
- (3) J. Zhao and Z. Chen, *J. Am. Chem. Soc.* 2017, **139** (36), 12480-12487.
- (4) W. Zhao, L. Zhang, Q. Luo, Z. Hu, W. Zhang, S. Smith and J. Yang, *ACS Catal.* 2019, **9** (4), 3419-3425.
- (5) X. Zhao and Y. Liu, *J. Am. Chem. Soc.* 2021, **143**, 9423–9428.
- (6) H. Liu, J. Liu and B. Yang, *ACS Catal.* 2021, **11** (19), 12336-12343.
- (7) S. Trasatti, *Pure Appl. Chem.*, 1986, **58**, 955–966.
- (8) K. Chan and J. K. Nørskov, *J. Phys. Chem. Lett.*, 2015, **6**, 2663–2668.